PHYSICAL REVIEW C **88**, 041307(R) (2013)

Simple correlations between electric quadrupole moments of atomic nuclei

J. M. Allmond
Joint Institute for Heavy Ion Research, Oak Ridge National Laboratory, Oak Ridge, Tennessee 37831, USA
(Received 10 July 2013; revised manuscript received 3 September 2013; published 31 October 2013)

Measurements of nonyrast electric quadrupole moments (i.e., diagonal $E2$ matrix elements) of atomic nuclei are becoming widely available from multiple-step Coulomb excitation. It is shown that, where quadrupole-moment data exist, $\langle 2_1^+||E2||2_1^+\rangle + \langle 2_2^+||E2||2_2^+\rangle \approx 0$ is observed across a wide range of masses, deformations, and first 2^+ energies. Nearly all of these quadrupole-moment data, particularly $\langle 2_2^+||E2||2_2^+\rangle$, are from the past two decades with half of the data from the past decade. In addition, $\langle 4_1^+||E2||4_1^+\rangle + \langle 4_2^+||E2||4_2^+\rangle + \langle 4_3^+||E2||4_3^+\rangle \approx 0$ is observed within two standard deviations for three of the four existing measurements. Despite many and varying complexities in the structure details of the individual nuclei, the correlations in the quadrupole moments appear simple.

DOI: 10.1103/PhysRevC.88.041307 PACS number(s): 21.10.Ky, 21.60.−n

Atomic nuclei are unique among finite many-body quantum systems (e.g., molecules, atomic clusters, ultracold monotonic gas condensates) in that electromagnetic moments can be measured through Coulomb excitation [1]. In particular, nuclei exhibit nonzero diagonal $E2$ matrix elements, $\langle I^\pi||E2||I^\pi\rangle$. It is shown that the electric quadrupole moments of atomic nuclei exhibit surprisingly simple correlations. In particular, $\langle 2_1^+||E2||2_1^+\rangle + \langle 2_2^+||E2||2_2^+\rangle$ and $\langle 4_1^+||E2||4_1^+\rangle + \langle 4_2^+||E2||4_2^+\rangle + \langle 4_3^+||E2||4_3^+\rangle$ are found to be approximately zero across a wide range of masses, deformations, and first 2^+ energies.

Table I shows all the available experimental $\langle 2^+||E2||2^+\rangle$ matrix elements for nuclei that have the first two $I^\pi = 2^+$ diagonal $E2$ matrix elements measured [2–21]. Ninety percent of these data are from the past two decades and nearly half of these data are from the past decade. The electric quadrupole-moment data show two distinct classes: (1) nuclei for which $\langle 2_1^+||E2||2_1^+\rangle$ and $\langle 2_2^+||E2||2_2^+\rangle$ have the opposite sign (i.e., 24 of the 28 nuclei) and (2) nuclei for which the signs are the same (i.e., 4 of the 28 nuclei). The nuclei for which the first and second 2^+ quadrupole moments have opposite sign show a relatively simple pattern in that they are, on average, equal in magnitude. The nuclei for which the quadrupole moments have the same sign (e.g., ^{148,150}Nd) are known to have 2_2^+ states associated with intrinsic $K^\pi = 0^+$ excitations [14,15]. This is a relatively rare exception for 2_2^+ states and they fall outside of the correlations presented in this study. While the situation for ^{68}Zn is similar to that of ^{148,150}Nd, ^{76}Kr (and less obviously ^{74,76}Kr) is complicated by shape coexistence of both prolate and oblate structures [9]. The 2_2^+ states in the krypton isotopes currently appear rather ambiguous with respect to $K^\pi = 0^+$ candidate assignments. Therefore, these nuclei are omitted in future discussion but are provided in Table I for completeness and scope.

Figure 1 shows the first and second 2^+ quadrupole-moment data plotted against (a) the atomic number Z, (b) the first 2^+ energy [22], (c) the ratio of the first 4^+ and 2^+ energies [22], and (d) the ground to first 2^+ $E2$ transition strength [2–21]. The 2_2^+ quadrupole moments mirror the 2_1^+ quadrupole moments with mass, energy, and transition strength.

Figure 1(a) shows that the 2_2^+ quadrupole moments equally indicate the proton shell closures; there appears to be an exception for the 2_2^+ state of ^{114}Cd at $Z = 48$ (more on this later). Figure 1(b) indicates that the 2_1^+ and 2_2^+ quadrupole moments remain correlated with first 2^+ energies, and Fig. 1(c) indicates that the correlation is maintained as one moves from the symmetric-rotor $E(4_1^+)/E(2_1^+) = 3.33$ limit towards the harmonic-vibrator $E(4_1^+)/E(2_1^+) = 2$ limit [23]. However, the harmonic-vibrator limit is never reached for the nuclei presented here. Instead, they appear to approach a grouping of $E(4_1^+)/E(2_1^+)$ ratios between 2.4 and 2.6, often associated with γ-soft and/or triaxial rotors. Furthermore, the two quadrupole moments are shown to be inversely proportional to the first 2^+ energy, which is similar to the experimental Grodzins correlation [24], $B(E2;0_1^+ \rightarrow 2_1^+)(e^2b^2) \approx 16\,Z^2/A\,E(2_1^+)$, where $E(2_1^+)$ is in units of keV and $B(E2;0_1^+ \rightarrow 2_1^+) = \langle 0_1^+||E2||2_1^+\rangle^2$. The inverse correlation between the first 2^+ energy and the $\langle 0_1^+||E2||2_1^+\rangle$, $\langle 2_1^+||E2||2_1^+\rangle$, and $\langle 2_2^+||E2||2_2^+\rangle$ matrix elements are most likely related. This is supported by the near linear relationship between the transition and diagonal matrix elements shown in Fig. 1(d). The symmetric rotor predicts a simple constant relationship for these matrix elements (i.e., parameters free) and is shown by the solid lines. Conversely, the harmonic vibrator predicts the quadrupole moments to be zero (but not an anharmonic vibrator, which is not parameter free). A simple phenomenological fit of $|\langle 2_{1,2}^+||E2||2_{1,2}^+\rangle|(\text{eb}) = 235/E(2_1^+)$ is determined from the data in Fig. 1(b) with a quality of $R^2 = 0.93$ or equivalently, $|Q(2_{1,2}^+)|(\text{eb}) = 178/E(2_1^+)$, where $E(2_1^+)$ is in units of keV. A slightly better fit, which is more consistent with the Grodzins correlation (except for the nonzero offset), can be achieved with two parameters, $|\langle 2_{1,2}^+||E2||2_{1,2}^+\rangle|(\text{eb}) = 33/\sqrt{E(2_1^+)} - 0.97$ and $R^2 = 0.94$ for $E(2_1^+) < 1090$ keV (zero otherwise).

Figure 2 further illustrates the simple $\langle 2_1^+||E2||2_1^+\rangle + \langle 2_2^+||E2||2_2^+\rangle \approx 0$ correlation, as indicated by the uniform scatter of the data about the diagonal line, and it is shown to be maintained across a wide range of masses and deformations. A fit to the data gives $\langle 2_2^+||E2||2_2^+\rangle = -\langle 2_1^+||E2||2_1^+\rangle + 0.103$ with a quality of $R^2 = 0.93$.

TABLE I. Experimental $\langle 2^+||E2||2^+\rangle$ (eb) matrix elements and their summation, Σ.

	^{68}Zn[a,b] [2]	^{70}Ge[a] [3]	^{72}Ge [4]	^{74}Ge [5]	^{76}Ge [6]	^{76}Se [7]	^{78}Se [8]	^{80}Se [7]	^{82}Se [7]	
2_1^+	$0.12(^{+4}_{-4})$	$0.05(^{+4}_{-4})$	$-0.16(^{+10}_{-7})$	$-0.25(^{+3}_{-3})$	$-0.18(^{+5}_{-5})$	$-0.45(^{+7}_{-7})$	$-0.26(^{+9}_{-9})$	$-0.26(^{+4}_{-3})$	$-0.30(^{+4}_{-3})$	
2_2^+	$0.12(^{+8}_{-8})$	$-0.09(^{+5}_{-5})$	$0.30(^{+10}_{-0})$	$0.34(^{+8}_{-8})$	$0.37(^{+8}_{-8})$	$0.24(^{+6}_{-8})$	$0.22(^{+12}_{-12})$	$0.53(^{+3}_{-3})$	$0.45(^{+4}_{-5})$	
Σ	$0.24(^{+9}_{-9})$	$-0.04(^{+7}_{-7})$	$0.14(^{+14}_{-7})$	$0.09(^{+8}_{-8})$	$0.18(^{+10}_{-10})$	$-0.21(^{+9}_{-11})$	$-0.04(^{+15}_{-15})$	$0.27(^{+5}_{-4})$	$0.15(^{+6}_{-6})$	
	^{74}Kr[b] [9]	^{76}Kr[b] [9]	^{78}Kr[b] [10]	^{106}Pd [11]	^{108}Pd [11]	^{110}Pd [12]	^{114}Cd [13]	^{148}Nd[b] [14]	^{150}Nd[b] [15]	
2_1^+	$-0.70(^{+33}_{-30})$	$-0.9(^{+3}_{-3})$	$-0.80(^{+4}_{-4})$	$-0.72(^{+6}_{-7})$	$-0.81(^{+4}_{-9})$	$-0.87(^{+17}_{-15})$	$-0.36(^{+1}_{-3})$	$-1.85(^{+4}_{-5})$	$-2.265(^{+40}_{-80})$	
2_2^+	$0.33(^{+28}_{-23})$	$-1.0(^{+5}_{-5})$	$0.58(^{+4}_{-8})$	$0.52(^{+6}_{-5})$	$0.73(^{+9}_{-7})$	$0.70(^{+9}_{-32})$	$0.92(^{+4}_{-5})$	$-1.15(^{+8}_{-12})$	$-0.766(^{+40}_{-81})$	
Σ	$-0.37(^{+43}_{-38})$	$-1.90(^{+58}_{-58})$	$-0.22(^{+6}_{-9})$	$-0.20(^{+8}_{-9})$	$-0.08(^{+10}_{-11})$	$-0.17(^{+19}_{-35})$	$0.56(^{+4}_{-6})$	$-3.00(^{+9}_{-13})$	$-3.03(^{+6}_{-11})$	
	^{166}Er [16]	^{168}Er [17]	^{182}W [18]	^{184}W [18]	^{186}Os [19]	^{188}Os [19]	^{190}Os [19]	^{192}Os [19]	^{194}Pt[a] [20]	^{196}Pt[a] [21]
2_1^+	$-2.33(^{+19}_{-12})$	$-3.25(^{+10}_{-25})$	$-2.00(^{+4}_{-8})$	$-1.97(^{+6}_{-4})$	$-1.75(^{+22}_{-13})$	$-1.73(^{+19}_{-5})$	$-1.25(^{+22}_{-13})$	$-1.21(^{+6}_{-17})$	$0.61(^{+6}_{-6})$	$0.82(^{+10}_{-10})$
2_2^+	$2.97(^{+17}_{-15})$	$2.85(^{+9}_{-9})$	$1.94(^{+10}_{-4})$	$2.36(^{+11}_{-5})$	$2.12(^{+6}_{-22})$	$2.10(^{+9}_{-6})$	$1.53(^{+6}_{-31})$	$0.985(^{+45}_{-85})$	$-0.66(^{+14}_{-14})$	$-0.52(^{+20}_{-20})$
Σ	$0.64(^{+25}_{-19})$	$-0.40(^{+13}_{-27})$	$-0.06(^{+11}_{-9})$	$0.39(^{+13}_{-6})$	$0.37(^{+23}_{-26})$	$0.37(^{+21}_{-8})$	$0.28(^{+23}_{-34})$	$-0.23(^{+8}_{-19})$	$-0.05(^{+15}_{-15})$	$0.30(^{+22}_{-22})$

[a]Nucleus is oblate in shape.
[b]2_2^+ associated with $K^\pi = 0^+$.

The simplest model that is consistent with the experimental observation of $\langle 2_1^+||E2||2_1^+\rangle + \langle 2_2^+||E2||2_2^+\rangle \approx 0$ follows from the quadrupole moments of rotor models (see Bohr and Mottelson [23] and Rowe and Wood [25]). In the simplest form, the diagonal reduced $E2$ matrix elements are given by

$$\langle IK||E2||IK\rangle = Q_0\sqrt{\frac{5}{16\pi}}\sqrt{2I+1}\langle IK;20|IK\rangle \text{ (eb)} \quad (1)$$

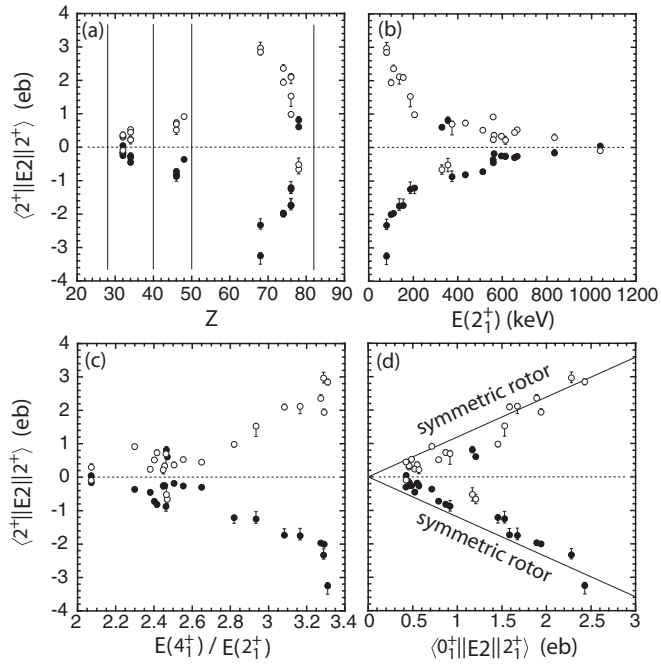

FIG. 1. The $\langle 2_1^+||E2||2_1^+\rangle$ and $\langle 2_2^+||E2||2_2^+\rangle$ matrix elements from Table I are plotted together as functions of (a) the atomic number Z, (b) the first 2^+ energy, (c) the ratio of the first 4^+ and 2^+ energies, and (d) the ground to first 2^+ $E2$ transition strength, where $\langle 0_1^+||E2||2_1^+\rangle = \sqrt{B(E2;0^+ \to 2^+)}$. The solid circles are for 2_1^+ and the open circles are for 2_2^+.

and the corresponding static quadrupole moments are given by

$$Q(IK) = \sqrt{\frac{16\pi}{5}}\frac{\langle II;20|II\rangle}{\sqrt{2I+1}}\langle IK||E2||IK\rangle \text{ (eb)}$$
$$= Q_0\frac{3K^2 - I(I+1)}{(I+1)(2I+3)} \text{ (eb)}, \quad (2)$$

where I is the total angular momentum, K is the projection of the total angular momentum onto the body-frame symmetry axis, and the parameter Q_0 is the intrinsic electric quadrupole deformation.

Within the rotor model, if the first two 2^+ states are described by $K^\pi = 0^+$ and 2^+, then

$$\langle 2_1^+||E2||2_1^+\rangle + \langle 2_2^+||E2||2_2^+\rangle$$
$$= Q_0\sqrt{\frac{5}{16\pi}}\sqrt{2(2)+1}\{\langle 20;20|20\rangle + \langle 22;20|22\rangle\} = 0, \quad (3)$$

where $\langle 20;20|20\rangle = -\langle 22;20|22\rangle$. In the limit of the rigid triaxial rotor (i.e., rigid axially asymmetric rotor), these are the only two $I^\pi = 2^+$ states in the model space. The theoretical relationship $\langle 2_1^+||E2||2_1^+\rangle + \langle 2_2^+||E2||2_2^+\rangle = 0$ is widely known for rotor models (but not the scope and widespread occurrence of the data). For example, the rigid triaxial rotor model [26,27] and the axially symmetric β-rigid γ-vibrator rotor model [28,29] both give this relationship, which highlights, in part, the difficulty in differentiating between the two different structures. The possibility of shape coexistence [30] further complicates this distinction. In addition, the SU(3) model, which provides a more microscopic perspective, gives similar results [31]. This is to be expected because the SU(3) model contracts to the triaxial rigid rotor model in a large-dimensional limit (i.e., large λ and μ).

While the 2^+ quadrupole-moment data seem to be consistent with the prediction of the rotor model, this does not necessarily mean or imply that these nuclei are rotors. The

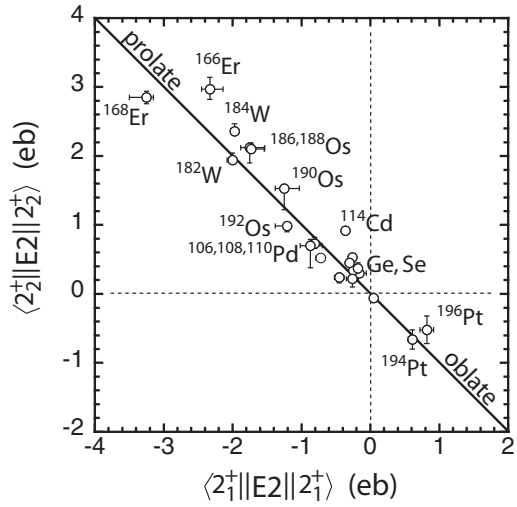

FIG. 2. The $\langle 2_1^+||E2||2_1^+\rangle$ and $\langle 2_2^+||E2||2_2^+\rangle$ matrix elements from Table I are plotted against each other. Data points on the solid 45° line give $\langle 2_1^+||E2||2_1^+\rangle + \langle 2_2^+||E2||2_2^+\rangle = 0$.

rotor model provides a simple, parameter-free starting point in which one might begin to understand the simple patterns observed in the data. Indeed, rotor models do not explain all the patterns of the low-lying states of these nuclei, which is why, in part, the widespread occurrence of the quadrupole-moment correlations are surprising.

To broaden the scope of the theoretical discussion, calculations within the interacting boson model [32] (IBM) were carried out with the IBM1 fortran code from Van Isacker [33] using the simple Hamiltonian of Ref. [34] with consistent-Q formalism between the Hamiltonian and the $E2$ operator. The IBM contains both spherical-vibrator and deformed-rotor limits. IBM1 calculations in general require various combinations of parameters to fit experimental data. However, a few generalities can be stated about its ability to reproduce the 2^+ quadrupole-moment correlations that pertain to all of its limits without going into optimal parameter sets and calculations. In short, $\langle 2_1^+||E2||2_1^+\rangle + \langle 2_2^+||E2||2_2^+\rangle \approx 0$ can be explained within the framework of the IBM1. However, the idealization of a zero sum can only be reached exactly within the IBM1 when large boson numbers are used. For finite boson number, the IBM1 predicts that $\langle 2_1^+||E2||2_1^+\rangle$ is always greater in magnitude than $\langle 2_2^+||E2||2_2^+\rangle$. This feature of the IBM1 implies that the 2^+ quadrupole-moment data should fall to one side of the diagonal line in Fig. 2, as opposed to being scattered uniformly about it. In particular, the data should fall on or below the diagonal line for prolate nuclei and on or above the diagonal line for oblate nuclei. However, shape coexistence between two IBM1 subspaces could alter this prediction.

A detailed survey of the individual nuclei that make up the 2^+ quadrupole-moment data reveals various complexities and seemingly contradictory interpretations. Despite these complexities, the correlations in the 2^+ quadrupole moments appear simple. A detailed discussion of the various nuclei that make up the 2^+ quadrupole-moment data are in order, which are discussed from smallest to largest quadrupole moments (cf. Fig. 2).

The nuclei with the smallest quadrupole moments in Fig. 2 are from the Ge and Se isotopes. Evidence for rigid triaxiality in the Ge region has recently been presented for ^{76}Ge through the use of energy and γ-ray branching-ratio patterns [35]. This study has been highlighted as the best manifestation of rigid triaxiality. For instance, the experimental ratio of $E(4_1^+)/E(2_1^+) = 2.51$ [22] is close to the 2.67 ratio [26] expected for a triaxial rotor at $\gamma = 30°$. Observation of the static quadrupole-moment sum, $\langle 2_1^+||E2||2_1^+\rangle + \langle 2_2^+||E2||2_2^+\rangle = 0.18(10)$ eb (cf. Table I and Fig. 2), reveals consistency with zero to within two standard deviations; this is also true for the other Ge isotopes. The rather small quadruple moments for a rigid deformed triaxial rotor can be justified as a destructive interference effect between the inertia and electric quadrupole tensors [36]. The neighboring Se isotopes are also interesting for further investigations of triaxiality. However, this entire region is potentially complex, which has been highlighted by a recent multiple-step Coulomb-excitation study of the nearby Kr isotopes [9], providing evidence for shape-coexisting triaxiality.

The Cd and Pd region, which shows similar quadrupole-moment magnitudes as the Pt isotopes, has traditionally been considered vibrational-like based on energy patterns (cf. Ref. [37] and references therein) and are typically considered textbook examples of vibrations. In particular, ^{118}Cd played a key role in the establishment of the U(5) limit of the IBM [37], which has quadrupole moments of zero in the strict limit. However, there has recently been significant evidence against a vibrational interpretation of this region [38–44], which has $E2$ transition patterns that mimic quasirotational behavior. The relatively low-lying deformed intruder states in the Cd isotopes further complicate the interpretation of the structure owing to potential mixing. The 2^+ quadrupole moments for the Pd isotopes, which are relatively large with uncertainties that are better than 20% for all but one quadrupole moment in ^{110}Pd, show (cf. Table I and Figs. 1 and 2) remarkable consistency with a zero sum. For ^{114}Cd, $\langle 2_1^+||E2||2_1^+\rangle + \langle 2_2^+||E2||2_2^+\rangle$ is not near zero but it is interesting to note that the first and second 2^+ states have nonzero quadrupole moments (better than 11% precision) that are opposite in sign. Fahlander *et al.* [13], who measured the second 2^+ quadrupole moment, suggested that the 2_2^+ state appears to be a quasi-γ bandhead, as opposed to a two-phonon vibration member. A persistence of deformed, rotational-like $E2$ character in these nuclei (and others) is also supported from shape-invariant studies by Kumar and Cline [45] (see also Ref. [46]) using transition $E2$ matrix elements. For a more global view of nuclei containing rotational-like $E2$ character with vibrational-like energy patterns, see Refs. [47,48].

Additional $\langle 2_2^+||E2||2_2^+\rangle$ matrix-element measurements for the other Cd isotopes may provide valuable insight into the underlying structure of these seemingly complex nuclei, particularly for the neutron-rich and proton-rich isotopes where the 2^+ intruder levels are much higher in excitation energy (i.e., less potential mixing with the 2_1^+ and 2_2^+ states). In general, measurements for nuclei just above and below $Z = 50$ (and about other closed shells), where collectivity and deformation begin to emerge, would be of particular interest.

TABLE II. Experimental $\langle 4^+||E2||4^+\rangle$ (eb) matrix elements and their summation, Σ.

	^{186}Os [19]	^{188}Os [19]	^{190}Os [19]	^{192}Os [19]
4_1^+	$-2.02(^{+39}_{-18})$	$-2.00(^{+9}_{-20})$	$-1.28(^{+27}_{-19})$	$-0.73(^{+26}_{-6})$
4_2^+	$-1.12(^{+25}_{-23})$	$-1.22(^{+16}_{-10})$	$-1.29(^{+20}_{-25})$	$-0.83(^{+9}_{-8})$
4_3^+	$2.35(^{+92}_{-69})$	$2.68(^{+22}_{-19})$	$1.02(^{+18}_{-4})$	$1.28(^{+15}_{-41})$
Σ	$-0.79(^{+103}_{-75})$	$-0.54(^{+29}_{-29})$	$-1.55(^{+38}_{-32})$	$-0.28(^{+31}_{-42})$

The Pt and Os region is commonly considered characteristic of γ-soft and/or triaxial rotors [19,20,36,49–57], with nuclei at or near a prolate-oblate shape transition and $E(4_1^+)/E(2_1^+)$ ratios ranging from 2.47 to 3.16. In particular, ^{196}Pt played a key role in the introduction of the O(6) limit of the IBM via a study of energy and γ-decay branching patterns of this nucleus [54]. The strict O(6) limit of the IBM gives $\langle 0_1^+||E2||2_2^+\rangle = 0$ and $\langle 2_{1,2}^+||E2||2_{1,2}^+\rangle = 0$ as a consequence of the O(6) boson dynamical symmetry (i.e., a selection rule). The rigid triaxial rotor of Davydov and Filippov [26] gives a similar result for a triaxiality of $\gamma = 30^\circ$. However, ^{196}Pt has nonzero quadrupole moments where $\langle 2_1^+||E2||2_1^+\rangle + \langle 2_2^+||E2||2_2^+\rangle$ is consistent with zero. Recently, it was shown [36] that the $E2$ properties of the 2_1^+ and 2_2^+ states are consistent with a destructive interference effect in a recently formulated version of the rigid triaxial rotor model [27], which relaxes the irrotational flow condition of the Davydov and Filippov model [26], providing the possibility of $\langle 0_1^+||E2||2_2^+\rangle = 0$ and $\langle 2_{1,2}^+||E2||2_{1,2}^+\rangle \neq 0$.

The W and Er isotopes represent traditional rotational-like nuclei, as is evident from their relatively large electric quadrupole moments and energy ratios of $E(4_1^+)/E(2_1^+) \sim 3.3$ [16–18]. The Er isotopes represent the closest idealization of the rotor, as was recently shown in a high-precision test in Ref. [58] using branching ratios from excited $K^\pi = 2^+$ states.

In light of the observed correlations in the 2^+ quadrupole moments, it is worth pursuing an attempt to search for correlations in 4^+ quadrupole moments. Table II shows all the available experimental $\langle 4^+||E2||4^+\rangle$ matrix elements for nuclei that have the first three $I^\pi = 4^+$ diagonal $E2$ matrix elements measured; there are no known $I^\pi = 3^+$ states with a nonzero static quadrupole moment. The data here are limited and only one study with four measurements on the stable Os isotopes was found [19]. The first observation is that the first two 4^+ quadrupole moments have the same sign and that the 4_3^+ quadrupole moment has the opposite sign. Three of the four quadrupole-moment sums are consistent with zero to within 2σ, out of which two are consistent with zero to within 1σ. The quadrupole-moment sum for ^{190}Os is not consistent with zero. Because the data are limited and do not span a wide range of masses and deformations, plots similar to those in Fig. 1 are not possible. The correlations of the 4^+ quadrupole-moment data are shown in Fig. 3.

The simplest model that is consistent with the experimental observation of $\langle 4_1^+||E2||4_1^+\rangle + \langle 4_2^+||E2||4_2^+\rangle + \langle 4_3^+||E2||4_3^+\rangle \approx 0$ follows from the quadrupole moments of rotor models; cf. Eqs. (1) and (2). Within the rotor model, if the first three 4^+ states are described by $K^\pi = 0^+, 2^+$, and 4^+, then

$$\begin{aligned}&\langle 4_1^+||E2||4_1^+\rangle + \langle 4_2^+||E2||4_2^+\rangle + \langle 4_3^+||E2||4_3^+\rangle \\ &= Q_0\sqrt{\frac{5}{16\pi}}\sqrt{2(4)+1}\{\langle 40;20|40\rangle + \langle 42;20|42\rangle \\ &\quad + \langle 44;20|44\rangle\} = 0, \end{aligned} \tag{4}$$

where $\langle 40;20|40\rangle + \langle 42;20|42\rangle = -\langle 44;20|44\rangle$. In the limit of the rigid triaxial rotor, these are the only three $I^\pi = 4^+$ states in the model space. The rigid triaxial rotor model and the axially symmetric β-rigid γ-vibrator rotor model equally describe these 4^+ quadrupole-moment sums [25,57], which highlights, in part, the difficulty in differentiating between the different structures. This zero-sum relationship for spin 4^+ was not previously recognized. It turns out that the quadrupole-moment sums for spin 2^+ and 4^+ are part of a more general rule that applies to all spins. For example, for sums over $K^\pi = 0^+, 2^+, 4^+, \ldots$,

$$\sqrt{\frac{5}{16\pi}}Q_0\sqrt{2I+1}\times\sum_{K=0}^{I}\langle IK;20|IK\rangle = 0, \tag{5}$$

where K is even (i.e., from reflection symmetry), $\langle IK;20|IK\rangle$ is positive for $I = K$, and $\langle IK;20|IK\rangle$ can be negative or positive for $I > K$.

The IBM1 (see earlier discussion and explanation of the calculations) can also explain the observed $\langle 4_1^+||E2||4_1^+\rangle + \langle 4_2^+||E2||4_2^+\rangle + \langle 4_3^+||E2||4_3^+\rangle \approx 0$ correlations. The idealization of a zero sum can only be reached exactly within the IBM1 when large boson numbers are used. For finite boson number, the IBM1 predicts that $\langle 4_1^+||E2||4_1^+\rangle + \langle 4_2^+||E2||4_2^+\rangle$ is always greater in magnitude than $\langle 4_3^+||E2||4_3^+\rangle$, which is consistent with the observed data (i.e., the data systematically fall below the diagonal line in Fig. 3).

^{190}Os is a clear outlier from $\langle 4_1^+||E2||4_1^+\rangle + \langle 4_2^+||E2||4_2^+\rangle + \langle 4_3^+||E2||4_3^+\rangle = 0$ and from the other Os isotopes in Fig. 3. A potential explanation comes from reports of large two-proton two-quasiparticle (hexadecapole) components in the 4_3^+ wave function [59–61] with the implication that there must exist another $|I^\pi = 4^+, K^\pi = 4^+\rangle$ state. Bagnell *et al.* [59] report a state at ~2600 keV in ^{190,192}Os that may contain the remaining two-quasiparticle component. More recently, a (^{3}He,d) transfer study by Phillips *et al.* [62] has found evidence for large $K^\pi = 4^+$ hexadecapole (two-proton two-quasiparticle) components in the 4_3^+ states of ^{186,188}Os. A second $|I^\pi = 4^+, K^\pi = 4^+\rangle$ prolate state would provide a positive quadrupole moment (i.e., it would contain the missing strength). Of ^{186,188,190,192}Os, ^{190}Os has been determined [62,63] to have the largest two-proton two-quasiparticle (hexadecapole) component in the 4_3^+ wave function. This complex character of low-lying $K^\pi = 4^+$ bands may be widely occurring [64].

Additional 4_3^+ quadrupole-moment measurements in other mass regions (e.g., $A \sim 110$ Ru and Mo isotopes) would be of high interest to see if correlations are maintained across a wide range of masses and deformations, such as those observed for the 2^+ quadrupole moments. In addition, $\langle 4_1^+||E2||4_1^+\rangle + \langle 4_2^+||E2||4_2^+\rangle + \langle 4_3^+||E2||4_3^+\rangle$ sums may provide a valuable tool in determining the degree to which

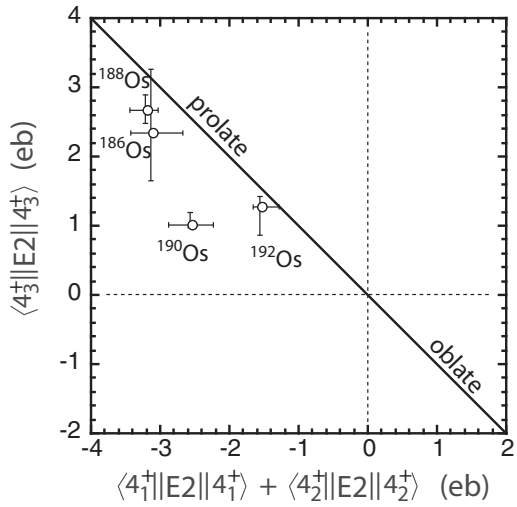

FIG. 3. The $\langle 4_1^+||E2||4_1^+\rangle + \langle 4_2^+||E2||4_2^+\rangle$ and $\langle 4_3^+||E2||4_3^+\rangle$ matrix elements from Table II are plotted against each other. Data points on the solid 45° line give $\langle 4_1^+||E2||4_1^+\rangle + \langle 4_2^+||E2||4_2^+\rangle + \langle 4_3^+||E2||4_3^+\rangle = 0$.

hexadecapole structures reside in low-lying 4^+ states. While 4_3^+ quadrupole moments are terribly difficult to measure, advancements in detector technology and efficiency, and sophisticated Coulomb-excitation codes (e.g., GOSIA [65]) make such measurements now feasible and should be sought.

In conclusion, it is shown that, where multiple-step Coulomb-excitation data exist, the sum of static quadrupole moments of atomic nuclei, particularly $\langle 2_1^+||E2||2_1^+\rangle + \langle 2_2^+||E2||2_2^+\rangle$, are remarkably consistent with zero across a wide range of masses, deformations, and first 2^+ energies, which include nuclei that have been traditionally considered vibrational-like from energy patterns. In addition, $\langle 4_1^+||E2||4_1^+\rangle + \langle 4_2^+||E2||4_2^+\rangle + \langle 4_3^+||E2||4_3^+\rangle \approx 0$ is observed within two standard deviations for three of the four existing measurements. The rotor model is the simplest model that is consistent with the experimental correlations observed in the static quadrupole moments. However, many of the nuclei are particularly complex and often exhibit contradictory signatures (e.g., energy patterns versus $E2$ matrix-element patterns). Despite these complexities, the correlations in the quadrupole moments appear simple. In a future study, it would be instructive to fully explore quadrupole-moment sum relationships in various models, including more realistic microscopic shell models. In light of these results, additional measurements of nonyrast electric quadrupole-moment data from multiple-step Coulomb excitation, particularly for 2^+ states in the Cd isotopes and 4^+ states in the Ru and Mo isotopes, could provide a better understanding of collectivity in the low-lying states of atomic nuclei and stimulate further theoretical investigation.

The author would like to thank D. G. Jenkins, T. Papenbrock, D. C. Radford, D. J. Rowe, A. E. Stuchbery, and J. L. Wood for fruitful discussions and useful comments on the manuscript. Research sponsored by the Office of Nuclear Physics, U.S. Department of Energy. The Joint Institute for Heavy Ion Research has as member institutions the University of Tennessee, Vanderbilt University, and the Oak Ridge National Laboratory; it is supported by the members and by the U.S. Department of Energy.

[1] K. Alder and A. Winther, *Coulomb Excitation* (Academic Press, New York, 1966).
[2] M. Koizumi *et al.*, Nucl. Phys. A **730**, 46 (2004).
[3] M. Sugawara, Eur. Phys. J. A **16**, 409 (2003).
[4] B. Kotliński *et al.*, Nucl. Phys. A **519**, 646 (1990).
[5] Y. Toh *et al.*, Eur. Phys. J. A **9**, 353 (2000).
[6] Y. Toh *et al.*, J. Phys. G: Nucl. Part. Phys. **27**, 1475 (2001).
[7] A. E. Kavka *et al.*, Nucl. Phys. A **593**, 177 (1995).
[8] T. Hayakawa *et al.*, Phys. Rev. C **67**, 064310 (2003).
[9] E. Clément *et al.*, Phys. Rev. C **75**, 054313 (2007).
[10] F. Becker *et al.*, Nucl. Phys. A **770**, 107 (2006).
[11] L. E. Svensson *et al.*, Nucl. Phys. A **584**, 547 (1995).
[12] L. E. Svensson, Ph.D. thesis, Uppsala University, 1989; L. Hasselgren *et al.*, University of Rochester Report No. NSRL-338, 1989.
[13] C. Fahlander *et al.*, Nucl. Phys. A **485**, 327 (1988).
[14] R. W. Ibbotson *et al.*, Nucl. Phys. A **619**, 213 (1997).
[15] N. Clarkson, Ph.D. thesis, University of Liverpool, 1992.
[16] C. Fahlander *et al.*, Nucl. Phys. A **537**, 183 (1992).
[17] B. Kotliński *et al.*, Nucl. Phys. A **517**, 365 (1990).
[18] C. Y. Wu *et al.*, Nucl. Phys. A **533**, 359 (1991).
[19] C. Y. Wu *et al.*, Nucl. Phys. A **607**, 178 (1996).
[20] J. M. Allmond, J. L. Wood, and W. D. Kulp, Phys. Rev. C **80**, 021303(R) (2009).
[21] C. S. Lim, R. H. Spear, M. P. Fewell, and G. J. Gyapong, Nucl. Phys. A **548**, 308 (1992).
[22] Evaluated Nuclear Structure Data File (ENSDF), http://www.nndc.bnl.gov/ensdf/.
[23] A. Bohr and B. R. Mottelson, *Nuclear Structure* (Benjamin, Reading, MA, 1975), Vol. II.
[24] L. Grodzins, Phys. Lett. **2**, 88 (1962).
[25] D. J. Rowe and J. L. Wood, *Fundamentals of Nuclear Models: Foundational Models* (World Scientific, Singapore, 2010).
[26] A. S. Davydov and G. F. Filippov, Nucl. Phys. **8**, 237 (1958).
[27] J. L. Wood, A-M. Oros-Peusquens, R. Zaballa, J. M. Allmond, and W. D. Kulp, Phys. Rev. C **70**, 024308 (2004).
[28] D. J. Rowe, Nucl. Phys. A **735**, 372 (2004).
[29] M. A. Caprio, Phys. Rev. C **83**, 064309 (2011).
[30] K. Heyde and J. L. Wood, Rev. Mod. Phys. **83**, 1467 (2011).
[31] R. Le Blanc, J. Carvalho, and D. J. Rowe, Phys. Lett. B **140**, 155 (1984).
[32] A. Arima and F. Iachello, Phys. Rev. Lett. **35**, 1069 (1975).
[33] P. Van Isacker, IBM1 code, unpublished.
[34] D. D. Warner and R. F. Casten, Phys. Rev. Lett. **48**, 1385 (1982).
[35] Y. Toh *et al.*, Phys. Rev. C **87**, 041304(R) (2013).
[36] J. M. Allmond, J. L. Wood, and W. D. Kulp, Phys. Rev. C **81**, 051305(R) (2010).
[37] A. Aprahamian, D. S. Brenner, R. F. Casten, R. L. Gill, and A. Piotrowski, Phys. Rev. Lett. **59**, 535 (1987).

[38] P. E. Garrett, K. L. Green, H. Lehmann, J. Jolie, C. A. McGrath, M. Yeh, and S. W. Yates, Phys. Rev. C **75**, 054310 (2007).
[39] P. E. Garrett, K. L. Green, and J. L. Wood, Phys. Rev. C **78**, 044307 (2008).
[40] J. C. Batchelder *et al.*, Phys. Rev. C **80**, 054318 (2009).
[41] P. E. Garrett and J. L. Wood, J. Phys. G: Nucl. Part. Phys. **37**, 069701 (2010).
[42] P. E. Garrett *et al.*, Phys. Rev. C **86**, 044304 (2012).
[43] J. C. Batchelder *et al.*, Phys. Rev. C **86**, 064311 (2012).
[44] F. M. Prados-Estevez *et al.* [Phys. Rev. C (to be published)].
[45] K. Kumar, Phys. Rev. Lett. **28**, 249 (1972); D. Cline, Ann. Rev. Nucl. Part. Sci. **36**, 683 (1986).
[46] W. Andrejtscheff and P. Petkov, Phys. Rev. C **48**, 2531 (1993).
[47] G. Thiamova, D. J. Rowe, and J. L. Wood, Nucl. Phys. A **780**, 112 (2006).
[48] J. Kern, P. E. Garrett, J. Jolie, and H. Lehmann, Nucl. Phys. A **593**, 21 (1995).
[49] J. E. Glenn, R. J. Pryor, and J. X. Saladin, Phys. Rev. **188**, 1905 (1969).
[50] H. L. Sharma and N. M. Hintz, Phys. Rev. Lett. **31**, 1517 (1973); Phys. Rev. C **13**, 2288 (1976).
[51] S. W. Yates *et al.*, Nucl. Phys. A **222**, 276 (1974); **222**, 301 (1974).
[52] I. Y. Lee, D. Cline, P. A. Butler, R. M. Diamond, J. O. Newton, R. S. Simon, and F. S. Stephens, Phys. Rev. Lett. **39**, 684 (1977).
[53] R. F. Casten and J. A. Cizewski, Nucl. Phys. A **309**, 477 (1978); **425**, 653 (1984).
[54] J. A. Cizewski, R. F. Casten, G. J. Smith, M. L. Stelts, W. R. Kane, H. G. Börner, and W. F. Davidson, Phys. Rev. Lett. **40**, 167 (1978).
[55] C. Y. Wu and D. Cline, Phys. Lett. B **382**, 214 (1996).
[56] C. Y. Wu *et al.*, Phys. Rev. C **64**, 014307 (2001).
[57] J. M. Allmond, R. Zaballa, A. M. Oros-Peusquens, W. D. Kulp, and J. L. Wood, Phys. Rev. C **78**, 014302 (2008).
[58] W. D. Kulp *et al.*, Phys. Rev. C **73**, 014308 (2006).
[59] R. D. Bagnell *et al.*, Phys. Lett. B **66**, 129 (1977); R. D. Bagnell, Y. Tanaka, R. K. Sheline, D. G. Burke, and J. D. Sherman, Phys. Rev. C **20**, 42 (1979).
[60] D. G. Burke *et al.*, Phys. Lett. B **78**, 48 (1978).
[61] F. T. Baker *et al.*, Nucl. Phys. A **501**, 546 (1989); **258**, 43 (1976).
[62] A. A. Phillips *et al.*, Phys. Rev. C **82**, 034321 (2010).
[63] D. G. Burke, Phys. Lett. B **406**, 200 (1997).
[64] D. G. Burke, Phys. Rev. Lett. **73**, 1899 (1994).
[65] T. Czosnyka *et al.*, Bull. Am. Phys. Soc. **28**, 745 (1983); http://www.pas.rochester.edu/∼cline/Gosia/.